

Polymerization and Crystallization Behavior of a LaRC-TPI Powder*

T. H. HOU,[†] J. M. BAI,[‡] and T. L. ST. CLAIR, *NASA Langley
Research Center, MS 226, Hampton, Virginia 23665-5225*

Synopsis

The crystallization and polymerization behavior of a crystalline LaRC-TPI powder at elevated temperatures have been studied. The characterization methods include differential scanning calorimetry and the measurements of inherent viscosity, η_{inh} , and viscoelastic properties of the fully imidized samples. The as-received material possesses an initial crystal melting peak temperature of 272°C. For the material annealed at temperatures below 320°C, a semicrystalline polymer can be obtained. On the other hand, a purely amorphous structure is realized in the samples annealed at temperatures above 320°C. Isothermal crystallization kinetics are studied by means of the simple Avrami equation. The likely nucleation path is attributed as an intermolecular oligomer nucleation type. The isothermal polymerization behavior is quantified by inherent viscosity measurements. A single cure is found to correlate values of T_g and η_{inh} for samples experiencing different thermal histories. Fully imidized amorphous and semicrystalline LaRC-TPI samples are successfully molded based on the information obtained from thermal analyses. The viscoelastic properties of these samples are also reported.

INTRODUCTION

LaRC-TPI (*Langley Research Center-Thermoplastic Polyimide*) is a linear aromatic polyimide. Since its discovery by NASA in the late 1970s,¹⁻⁵ this material has been developed for a variety of high temperature applications. In its fully imidized form, the LaRC-TPI can be used as an adhesive for bonding metals such as titanium, aluminum, copper, and stainless steel. Other applications⁶ include insulating film and composite resin matrix, and so on. It was noted, however, that the relatively poor flow characteristics for this polymer have limited the applications. The viscosity at approximately 100°C above its glass transition temperature is at the order of 10^5 – 10^6 Pa-s.

Under a licensing agreement between NASA and Mitsui Toatsu of Japan in an effort to make this high temperature thermoplastic available to the aerospace and electronics industries, a version of LaRC-TPI imidized molding powder was received from Mitsui Toatsu and evaluated in NASA. A melt endotherm was noted during calorimetric analysis. The extraordinary level of flow exhibited by the crystalline powder at melt had not been seen for any other versions of LaRC-TPI that had been examined. This melting characteristic could potentially enhance processability of the material in those applications where the viscosity is a critical variable.⁷

*Portions of this work were presented at SPE ANTEC 87, Los Angeles, CA.

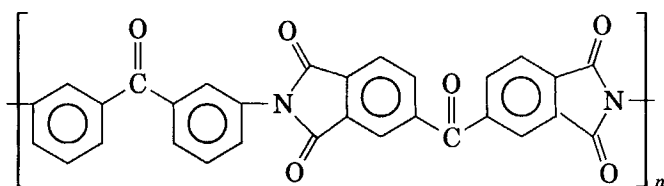
[†]T. H. Hou is a Unit Supervisor, PRC Kentron, Inc., Hampton, VA 23666.

[‡]J. M. Bai is a Graduate Student, Dept. Mechanical Engineering and Mechanics, Old Dominion University, Norfolk, VA 23508.

The thermal and rheological properties of this unusual form of LaRC-TPI have been briefly reported by Burks et al.⁸ A further study of the polymerization and crystallization behavior of LaRC-TPI and the kinetics of isothermal crystallization for this material are described in this paper. The characterization methods used include differential scanning calorimetry (DSC), the measurements of inherent viscosity, and the viscoelastic properties.

EXPERIMENTAL

The LaRC-TPI powders were prepared and supplied by Mitsui Toatsu Company, New York, NY. The material was from lot number 72-501 and was manufactured in Tokyo, Japan. The chemical structure of LaRC-TPI is



Thermal Properties

A Perkin-Elmer Differential Scanning Calorimeter (DSC) model DSC-2 was used. Samples (3–6 mg) of finely divided polymer were accurately weighed into aluminum sample holders on an analytical balance to 10^{-4} g. A stream of dry nitrogen was continuously flowing over the sample and the reference during measurements. The glass transition temperatures (T_g) and the crystalline melt temperatures (T_m) were determined directly from the thermogram for the samples treated under either isothermal or constant rate of cooling conditions. The exothermic energy of crystallization and the heat of fusion were measured using a planimeter to determine the areas under the respective peaks on the thermograms. The temperature and energy scales of the machine were calibrated in advance according to the melting points and melting energies of several standard reference compounds as suggested by the manufacturer.⁹

Inherent Viscosities

Inherent viscosities were measured by dissolving 0.5% of the material in *m*-cresol. The measurements were made at 35°C. Dissolutions of the materials in *m*-cresol required elevated temperatures, especially for those annealed samples with high molecular weights and/or crystallinities. This was accomplished by stirring solutions at reflux overnight.

Viscoelastic Properties

The viscoelastic properties of the fully imidized LaRC-TPI were measured on a Rheometrics System 4 Rheometer. Both purely amorphous and semi-crystalline samples were studied. The rectangular torsion mode in the System 4 was employed. Dimensions of the samples with rectangular shapes measured approximately $2.5 \times 0.5 \times 0.045$ inches. Strain imposed on the sample was

varied manually during the measurement so that the proper torque level could be maintained. Oscillatory frequency was held constant at 10 rad/s. Temperature scans were made at 4°C increments after a 4 minute thermal soak at each temperature. Measurements of the viscoelastic properties were taken at the end of each 4 minute soak. A slight tensional force was always exerted on the sample during the entire course of the temperature scan.

RESULTS AND DISCUSSION

The as-received LaRC-TPI powder was found to be crystalline by X-ray diffraction and DSC as reported earlier.⁸ The estimated level of crystallinity is about 48%, and the melting endotherm peak reaches a minimum at 272°C. Drying of the powder in a vacuum oven overnight at 100°C resulted in a weight loss of 1.5%. It was also found that less than 5% weight loss was recorded by thermogravimetric measurement during a temperature scan up to 400°C.

Overall Crystallization and Polymerization Behavior

The LaRC-TPI powder did not exhibit crystallization exotherms during a number of single thermal treatments of various conditions. When a sample was heated from room temperature, at a rate of 20°C/min, to several temperatures higher than 272°C (the initial crystalline melting peak of the as-received material), and followed by a rapid quench, neither the crystallization exotherm peaks present during the initial scan, nor the crystalline melting peaks present during the second scan after the quenching were evident. The glass transition temperatures (T_g), however, are found to increase with the higher temperatures employed during the thermal treatments above 272°C.

The crystallization and polymerization behaviors of the LaRC-TPI samples treated under isothermal conditions were investigated. As-received powder was first heated at a rate of 20°C/min from room temperature to a specified temperature above its initial melting point (272°C). After the completion of various holding times at the temperature, a rapid quench to ambient temperature followed. Subsequent thermograms were obtained by rescanning the quenched samples at a rate of 20°C/min from RT to 400°C. Typical thermograms obtained after various holding times at 300°C are shown in Figure 1. The characteristic of bimodal melting peaks was noted for most samples. Both peaks occur at temperatures higher than the annealing temperature (300°C). The bimodal feature becomes more evident as the annealing time becomes longer. Both melting temperatures at the peaks were also noted to increase with increasing annealing times. The differences between the two peak temperatures, however, remain nearly the same (approximately 10–12°C) and are independent of the length of annealing time. These features indicate that the bimodal melting characteristics observed are possibly due to the formation of different crystalline phases.

The thermograms obtained after various annealing times at 280°C and 320°C are shown in Figures 2 and 3, respectively. Characteristics similar to those discussed above for the sample annealed at 300°C are observed. In the case of 280°C annealing, three melting peaks are formed. The peak at the

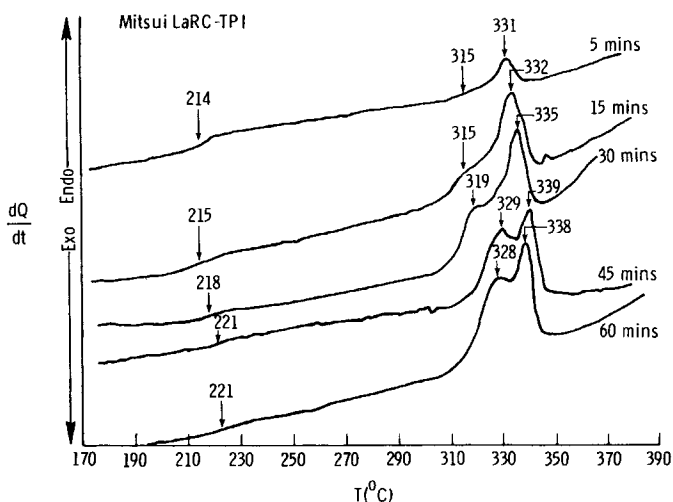


Fig. 1. DSC thermograms of the samples annealed at 300°C for various lengths of time.

highest temperature gradually becomes less evident as the annealing time becomes longer. The differences between peak temperatures, however, remain at 25 and 10°C, respectively. Only one melting peak is observed in Figure 3 for the sample annealed at 320°C.

Figure 4 is a direct comparison of crystallization characteristics for samples annealed for 60 minutes at the three temperatures indicated. It can be seen from Figures 1, 2, and 3 that for a 60 minute hold the crystallization processes are all nearly complete for these different isothermal conditions. Four distinct melting peaks are clearly identifiable from the figure. They are located in the vicinity of 300, 326, 336, and 350°C. The identification of crystalline forms formed at each temperature is a current research program.

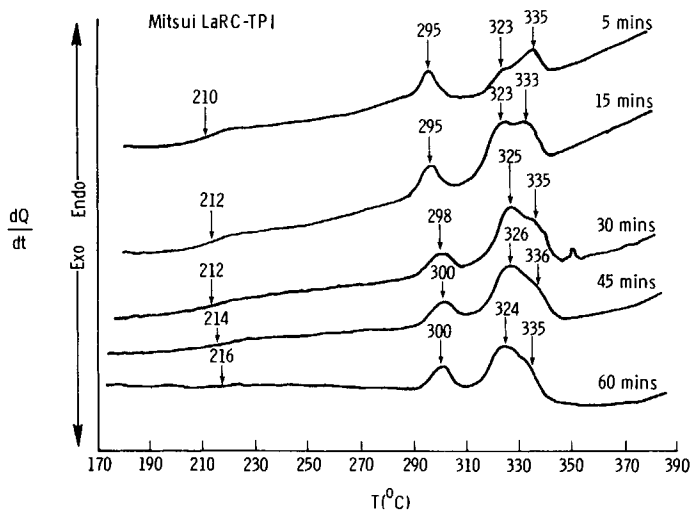


Fig. 2. DSC thermograms of the samples annealed at 280°C for various lengths of time.

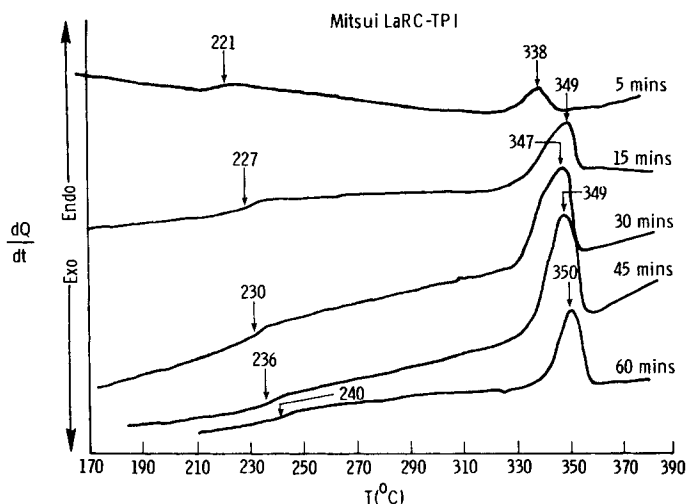


Fig. 3. DSC thermograms of the samples annealed at 320°C for various lengths of time.

The glass transition temperatures, T_g , are also seen from Figures 1, 2, and 3 to increase with increasing holding times at each annealing temperature. This is an indication that changes in both amorphous and crystalline regions occur at the same time during holds at the annealing temperatures below 320°C. The change in the amorphous region is likely due to chain extension and/or imide ring closure reactions. The increases in T_g and T_m as a function of hold time at each annealing temperature are plotted in Figures 5 and 6, respectively. In these figures the highest melting temperature is used for T_m . For different annealing conditions, both transition temperatures of the samples are seen to stabilize at different levels. In the case of T_g , values of 215, 220, and 240°C can be achieved in samples annealed for approximately 60 minutes

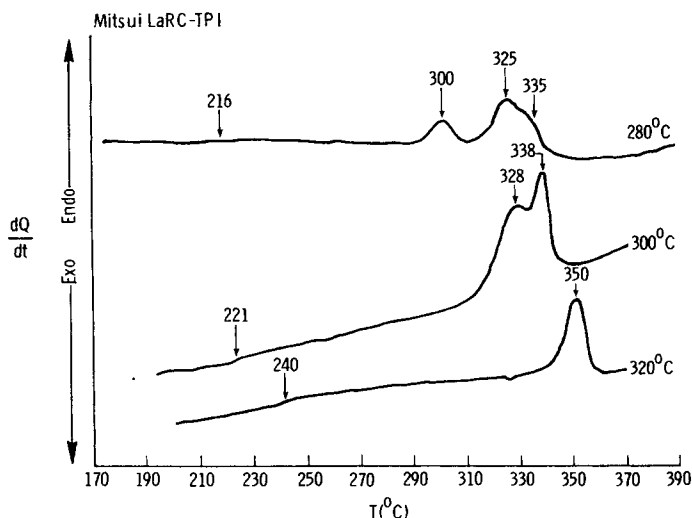


Fig. 4. DSC thermograms of three samples annealed for 60 minutes at three temperatures.

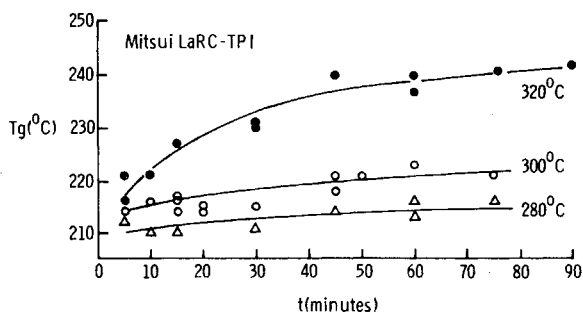


Fig. 5. The glass transition temperature $T_g(t)$ as a function of time for samples annealed at three temperatures. (●) 320°C; (○) 300°C; (△) 280°C.

at 280, 300, and 320°C, respectively. The highest attainable melt temperatures are also noted to be 325, 335, and 350°C, respectively, for samples annealed at 280, 300, and 320°C. Cross plots between $T_g(t)$ and $T_m(t)$ were made from Figures 5 and 6, and are shown in Figure 7. It is noted that crystallization is a dominant process for samples annealed at temperatures below 320°C. For an annealing temperature at 320°C, a chain extension polymerization reaction becomes dominant as evidenced by a higher rate of increase in T_g over T_m .

The overall crystallization and polymerization behaviors discussed above are observed only for the LaRC-TPI powder annealed isothermally at temperatures below 320°C. At annealing temperatures higher than 320°C, there are no crystalline melting peaks that can be detected. Only the chain extension polymerization reaction occurs as evidenced by the increase in $T_g(t)$ as a function of holding time. It is clear that for the material processed isothermally at temperatures at and below 320°C a semicrystalline structure can result. On the other hand, a purely amorphous structure is obtained when the as-received samples are processed isothermally at temperatures higher than 320°C.

The crystallization and chain extension polymerization behaviors for the LaRC-TPI samples treated under constant rate of cooling conditions were investigated. As-received powder was studied using DSC at a heating rate of 20°C/min from ambient temperature to a specified temperature above its initial melting point (272°C). A constant rate of cooling was then immediately employed until ambient temperature was regained. A subsequent thermogram

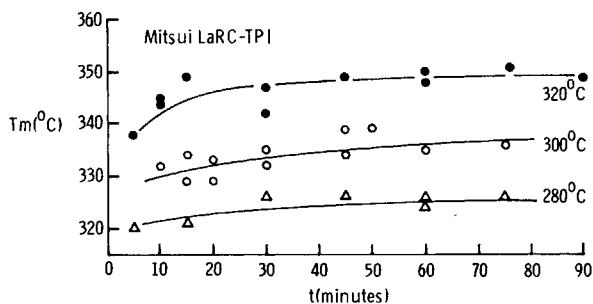


Fig. 6. The peak temperature of melt $T_m(t)$ as a function of time for samples annealed at three temperatures. (●) 320°C; (○) 300°C; (△) 280°C.

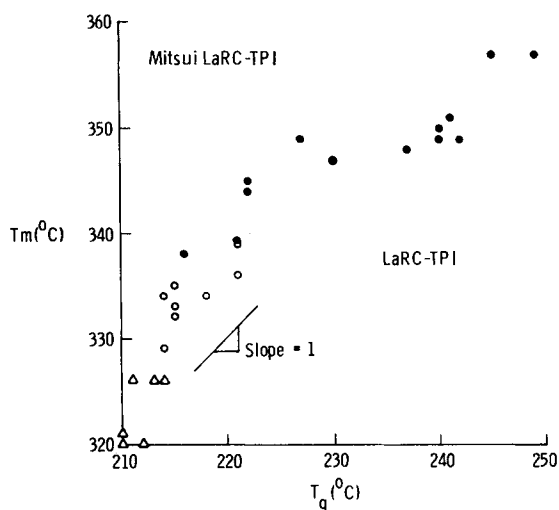


Fig. 7. Cross plot of $T_g(t)$ vs. $T_m(t)$ from Figures 5 and 6: (●) 320°C; (○) 300°C; (△) 280°C.

was obtained by rescanning the sample up to 400°C at a rate of 20°C/min. The thermograms obtained after cooling these samples from 300°C at various indicated rates are shown in Figure 8. As the cooling rate decreased, the characteristics of multiple melting behavior become more visible. This is also observed for samples cooled from 280 and 320°C, respectively. Figure 9 compares thermograms of samples cooled from various temperatures at a rate of 5°C/min. The overall behavior is quite different from that observed in isothermal annealing conditions discussed earlier. Multiple melting characteristics exist in all three cases in Figure 9. The highest melting temperature obtained in the sample by constant rates of cooling was lower than that obtained from isothermal annealing treatments.

It is also found that no crystalline melts were evident in the sample that was cooled at a constant rate from any temperature above 320°C. For the

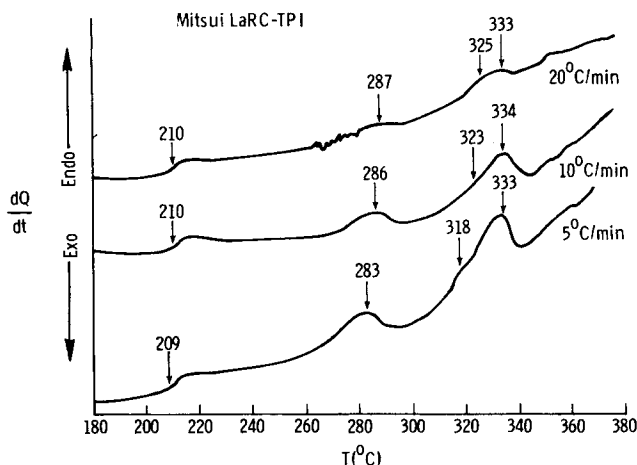


Fig. 8. DSC thermograms of samples annealed from 300°C with the constant rates of cooling.

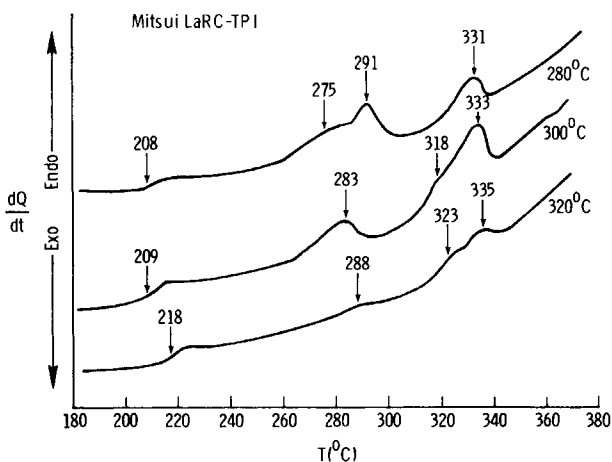


Fig. 9. DSC thermograms of the samples annealed with a cooling rate of 5°C/min from three temperatures.

polymers considered here, the C-C backbones are rather stiff. A likely nucleation path is, therefore, the intermolecular oligomer nucleation type.¹⁰ The major problem with the oligomer nucleation path lies in the initial formation of sufficient oligomer concentration for nucleation. A certain oligomer concentration must first be formed by a homogeneous reaction step before nucleation can occur and crystallization during polymerization can commence. The observations made above on the crystallization behavior under both conditions of isothermal annealing and constant rate of cooling suggest that at the elevated temperatures above 320°C, the polymerization reactions are so fast that the formation of crystallization nuclei with oligomers of sufficient concentration becomes less probable.

Kinetics of Isothermal Crystallization

Crystallization kinetics are commonly analyzed by means of the Avrami equation.^{10,11}

$$\chi_t = 1 - \exp(-Zt^n), \quad (1)$$

where χ_t is the weight fraction of crystallized material at time t , Z a rate constant, and n the Avrami exponent.

There is considerable doubt as to the validity of a simple Avrami equation alone describing the total crystallization behavior of bulk polymers. Despite this, however, analyses based upon Eq. (1) are justified, as a means of comparison, but the values of the parameters Z and n may have no mechanistic significances. Equation (1) can be rearranged as:

$$\text{Log}[-\text{Ln}(1 - \chi_t)] = \text{Log } Z + n \text{Log } t. \quad (2)$$

The Avrami parameters can then be conveniently extracted from the slope and intercept of the straight line in a plot of $\text{Log}[-\text{Ln}(1 - \chi_t)]$ vs. $\text{Log } t$.

Measurements of crystallization exotherms are restricted by the sensitivity of the calorimeter and the limit to sample size. For the LaRC-TPI powders

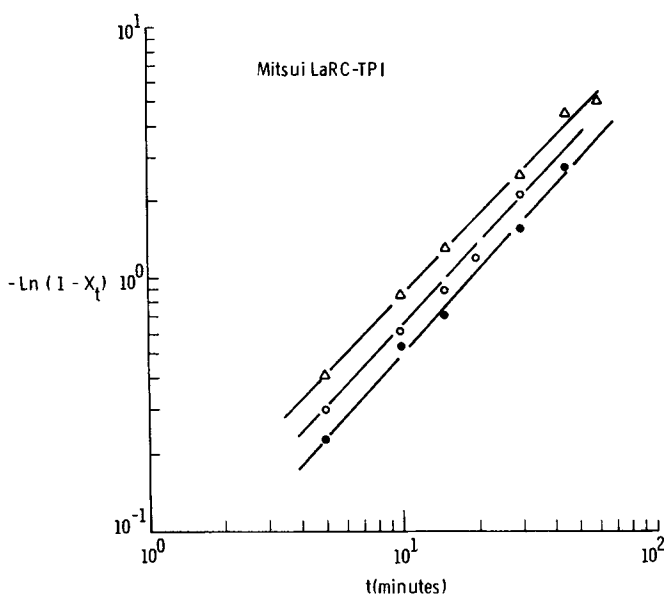


Fig. 10. Plots of Eq. (2) for the determination of Avrami parameters of crystallization for samples annealed isothermally: (●) 320°C; (○) 300°C; (△) 280°C.

studied here, the slow crystallization reaction rates make the crystallization exotherms difficult to trace. It is possible, however, to study the kinetics of crystallization by measuring the crystallinity developed in various time intervals from the area under the endotherms produced on the subsequent melting as shown by Figures 1, 2, and 3. This method is more time consuming and less accurate. It was reported, however, to give very similar crystallization isotherms to that of direct measurement in the study of polyethylene crystallization kinetics.¹²

Plots of Eq. (2) for the LaRC-TPI powders treated isothermally at three temperatures are shown in Figure 10. A straight line can be satisfactorily determined by the least-squares fit for each set of data. The Avrami parameters extracted from the fits are tabulated in Table I. It is noted that the n values are fractional but independent of annealing temperatures. The crystallization rate constant, Z , becomes smaller at higher temperature as expected from the earlier discussion.

Comparisons between Eq. (1) and the experimental data are shown in Figure 11. The agreements are considered satisfactory. It can be seen that among the three annealing temperatures studied here, $T = 300^\circ\text{C}$ is the most

TABLE I
Isothermal Crystallization Parameters for LaRC-TPI Powder

T ($^\circ\text{C}$)	n	$Z \times 10^2$ (min) $^{1/n}$
280	1.033	7.75
300	1.101	4.86
320	1.109	3.73

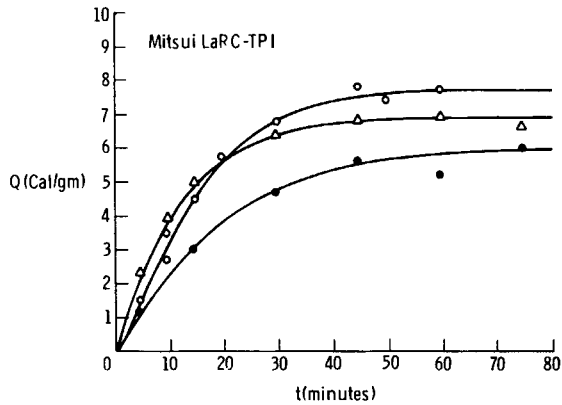


Fig. 11. Comparisons between experimental endothermic energies of fusion and time for samples annealed at three temperatures. (●) 320°C; (○) 300°C; (Δ) 280°C.

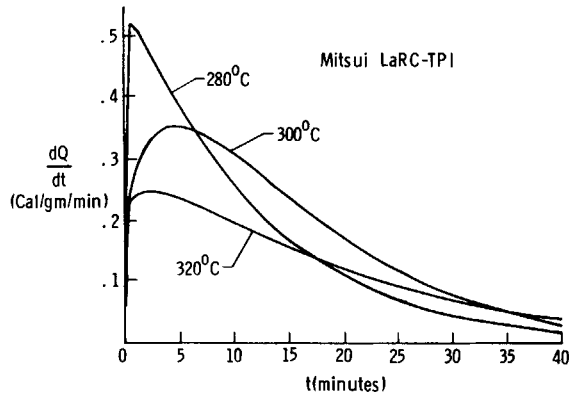


Fig. 12. Calculated exothermic values of crystallization as a function of time for samples annealed at the temperatures indicated.

favorable crystallization temperature for the material. The fastest crystallization reaction rate occurs, however, at 280°C as can be seen in this figure. The crystallization exotherms can be calculated by taking the derivative with respect to t in Eq. (1). The resultant exothermic curves are shown in Figure 12 for the three annealing temperatures indicated.

Isothermal Polymerization Behavior

The polymerization behavior of this material when annealed isothermally can be quantified by the measurements of inherent viscosities. Measurements were made on samples that had been annealed for various lengths of time at two temperatures shown in Figure 13. Samples annealed at 300°C were known to be semicrystalline. It is therefore not too surprising to note that the inherent viscosities quickly level off at $\eta_{inh} = 0.16$. The annealing temperature of 300°C favors crystallization reactions, as seen from the thermal analyses made above, and the polymerization reactions were hindered by this crystallization. The resultant samples that possess low molecular weights are related

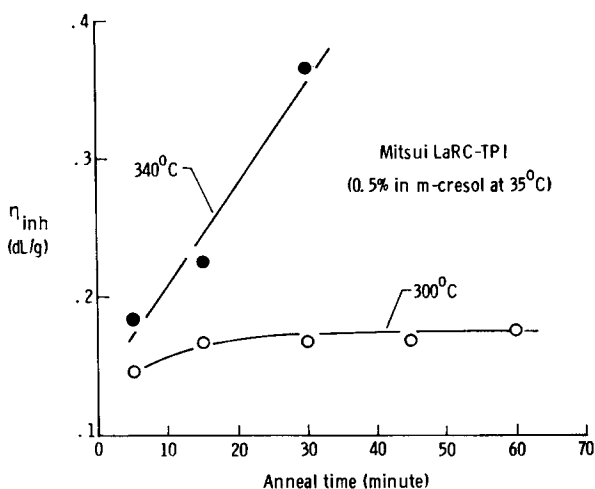


Fig. 13. Inherent viscosities of samples annealed for various lengths of time at the two temperatures shown: (●) 340°C; (○) 300°C.

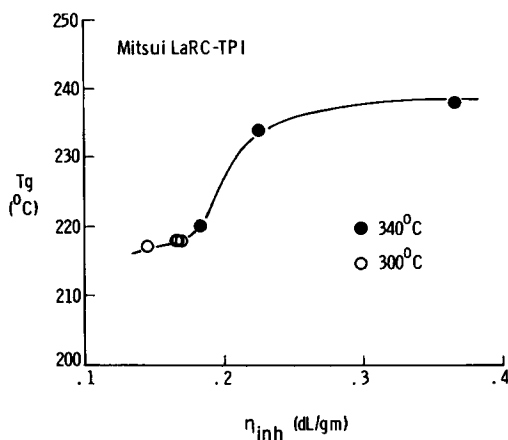


Fig. 14. Plot of T_g vs. η_{inh} for samples annealed for various lengths of time at the two temperatures shown: (●) 340°C; (○) 300°C.

to the relatively low level of T_g attainable in the materials under this annealing condition as shown earlier in Figure 5.

At 340°C anneal, purely amorphous materials can be realized. This annealing temperature favors polymerization reactions, and the fast increase in η_{inh} with the increase in annealing time is observed in Figure 13.

Plot of T_g vs. η_{inh} for samples annealed at various lengths of time is shown in Figure 14. It seems that all data points can be correlated with a single curve, despite the existence of structural differences in morphology among materials.

Viscoelastic Behavior

The complex modulus, G^* , measured by a Rheometrics System 4 Rheometer during a temperature scan at fixed frequency of 10 rad/s is shown in

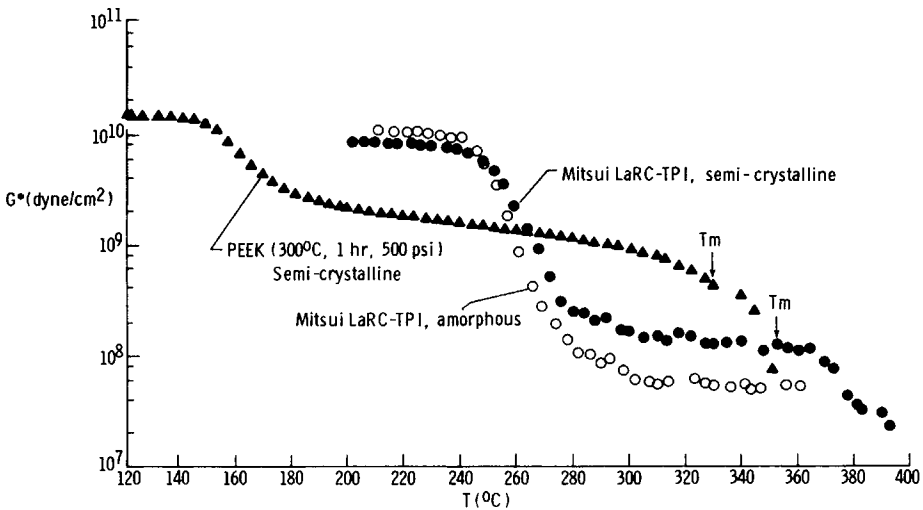


Fig. 15. Complex moduli of fully imidized LaRC-TPI and thermoplastic PEEK materials as a function of temperature.

Figure 15. Both amorphous and semicrystalline samples can be made by using different molding conditions, which were learned from the thermal analyses discussed above. The rectangular-shaped specimens were then cut from the 3" × 3" molded pieces. For the Mitsui LaRC-TPI samples, the temperature ranges in glass transition cover 40–60°C. Below the glass transition, the moduli are at a 1–2 × 10¹⁰ dyne/cm² level typical for such high performance materials. After the glass transition, moduli drop approximately two orders of magnitude. The higher modulus after T_g observed for the semicrystalline LaRC-TPI is attributed to the crystallinity in that sample.

It is known that crystallinity can enhance the solvent resistance of polymers. A high level of solvent resistance is crucial in aerospace applications. However, the use of crystalline materials above T_g offer the potential for catastrophic failure at T_m . It can be seen in Figure 15 that another significant drop in modulus occurs at temperatures higher than the crystal melting temperature of the semicrystalline sample.

The viscoelastic properties were also measured for the semicrystalline Poly(aryl-ether-ether-ketone) (PEEK) material as shown in the same figure. Several 3" × 3" pieces of PEEK of 0.010 inch in thickness were cut from a sheet of the polymer. The molding condition was at 300°C in temperature under 500 psi for 1 hour. A rectangular-shaped bar was then cut from the resultant molded piece which was semicrystalline, and the measurements were made. The material also showed a broad range in temperature during the glass transition. The difference in modulus after the glass transitions between semicrystalline PEEK and LaRC-TPI is attributed to different levels of crystallinity. The semicrystalline PEEK sample also exhibits another significant drop in modulus at temperatures higher than its crystal melting temperature, T_m . The glass transition temperature of PEEK, reported at 145°C, is seen to be significantly lower than the nominal T_g of 260°C possessed by the LaRC-TPI material.

CONCLUSIONS

The as-received crystalline LaRC-TPI powder is less readily crystallizable at temperatures above its initial melting point of 272°C when compared to other crystalline thermoplastics. Multiple crystal phases may be created in the samples with thermally different histories. These different crystal phases are readily identifiable from the DSC thermograms for samples annealed either isothermally or with a constant rate of cooling. The detailed morphological features of these crystal phases require further study. For the material annealed at temperatures below 320°C, a semicrystalline polymer can be obtained. On the other hand, a purely amorphous structure is realized in the samples annealed at temperatures above 320°C.

Isothermal crystallization kinetics were studied by means of the simple Avrami equation. The rate constants of crystallization were found to decrease with increasing annealing temperatures between 280 to 320°C. The Avrami exponent constants n for various experiments were found to be fractional and independent of annealing temperatures.

Results of inherent viscosity measurements on samples annealed at different temperatures for various lengths of time were found to be consistent with the thermal analyses. A single curve was used to correlate values of T_g and η_{inh} for samples experiencing different thermal treatments.

Processing conditions were identified based on the results of thermal analyses and the fully imidized amorphous and semicrystalline LaRC-TPI samples were successfully molded. Viscoelastic properties were measured for these high performance thermoplastic materials.

The authors would like to thank James R. Tyeryar, NASA Langley Research Center; and Joan Y. Z. Huang, the Old Dominion University, for their technical assistance during the course of this study.

References

1. V. L. Bell, B. L. Stump, and H. Gager, *J. Polym. Sci.*, **14**, 2275 (1976).
2. D. J. Progar, V. L. Bell, and T. L. St. Clair, NASA Langley Research Center, "Polyimide Adhesives," U.S. Patent 4,065,345 (1977).
3. V. L. Bell, NASA Langley Research Center, "Process for Preparing Thermoplastic Aromatic Polyimides," U.S. Patent 4,094,862 (1978).
4. A. K. St. Clair, L. T. Taylor, and T. L. St. Clair, NASA Langley Research Center, "Aluminum Ion-Containing Polyimide Adhesives," U.S. Patent 4,284,461 (1981).
5. A. K. St. Clair and T. L. St. Clair, NASA Langley Research Center, "High Temperatures Polyimide Film Laminates and Process for Preparation Thereof," U.S. Patent 4,543,295 (1985).
6. A. K. St. Clair and T. L. St. Clair, *SAMPE Qu.*, Oct 20-25 (1981).
7. N. J. Johnston and T. L. St. Clair, Proceedings 18th Internat. SAMPE Tech. Conf., pp. 53-67 (1986).
8. H. D. Burks, T. H. Hou, and T. L. St. Clair, *SAMPE Qu.*, **18-1**, 1-8 (1986).
9. Instructions Model DSC-2 Differential Scanning Calorimeter, Perkin-Elmer, Norwalk, CT (1979).
10. B. Wunderlich, *Macromolecular Physics*, Volume 2, Academic Press, New York, 1976.
11. T. Ozawa, *Polymer*, **12**, 150-158 (1971).
12. A. Booth and J. N. Hay, *Polymer*, **9** 95-103 (1968).

Received July 22, 1987

Accepted October 1, 1987